Mendeleev Communications

Mendeleev Commun., 2026, **36**, 37–40

Influence of N-heterocyclic carbene modification on the catalytic performance of Pd clusters and nanoparticles in the Mizoroki–Heck reaction

Alexander Yu. Kostyukovich,* Evgeniya S. Shutovskaya and Darya O. Prima

N. D. Zelinsky Institute of Organic Chemistry, Russian Academy of Sciences, 119991 Moscow, Russian Federation. E-mail: akos@ioc.ac.ru

DOI: 10.71267/mencom.7806

The addition of azolium salt as N-heterocyclic carbene (NHC) proligant improved the catalytic performance of palladium nanoparticles in the Mizoroki–Heck coupling. The catalytic activity of NHC-modified palladium on carbon (Pd-NHC/C) was evaluated in reactions involving a variety of olefin and aryl bromide counterparts. Quantum chemical calculations of the full reaction pathways for both ligand-free and NHC-modified Pd_2 clusters revealed a reduction in the activation energy of the second reaction route.

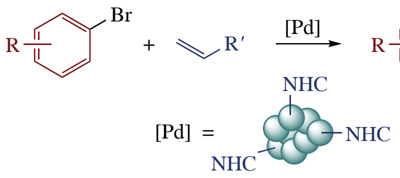

Keywords: modified nanoparticles, palladium clusters, reaction mechanism, palladium catalysis, Mizoroki–Heck reaction, DFT calculations.

Metal clusters and nanoparticles (NPs) are widely used in various fields of chemistry due to their large specific surface area and multifunctionality, which enables them to act as heterogeneous catalysts and to operate in homogeneous systems as sources of atomic metal.[1–4] Surface modification is an enticing tool for controlling the activity and the physicochemical properties of metal aggregates. Organic ligands used in metal complex catalysis can be good modifiers for metal surfaces.[5–7] For example, rhodium NPs modified with phosphine ligands were employed for the selective hydrogenation of aromatic compounds.[8]

An investigation of the evolution of highly efficient metal complex catalysts Pd/NHC revealed the formation of Pd nanoparticles through mechanisms of R-NHC and H-NHC coupling.[9–12] A detailed study of these nanoparticles, including chemical composition, catalytic properties, and behavior showed that they possessed catalytic activity in the Mizoroki–Heck, Suzuki–Miyaura, Buchwald–Hartwig, and Sonogashira reaction when their surface was modified with NHC ligands.[13]

Another possible approach to modify a metal surface involves the generation of free NHCs through deprotonation of the corresponding azolium salts.[5] This transformation can be carried out *in situ*, provided that the synthetic protocol assumes the presence of a sufficiently strong base in the reaction system. The Mizoroki–Heck reaction satisfies this condition and was chosen as a model system because it is one of the straightforward methods for the Pd-catalyzed synthesis of numerous substituted olefins.[14,15] Besides its high chemical importance, this reaction has a unique feature, namely, careful choice of conditions and substrates enables the reaction to proceed under homogeneous or heterogeneous catalysis, with or without ligands.

In this work, we investigated the effect of NHC-modification on the catalytic activity of Pd clusters and nanoparticles in the Mizoroki–Heck reaction. It was found that the addition of catalytic amount of azolium salt enhanced activity of commercially available palladium on carbon. A mechanistic explanation for this phenomenon was provided by quantum chemical calculations based on a simple model of a binuclear Pd cluster.

The positive effect of the azolium salt addition was demonstrated in the reaction between bromobenzene and styrene (Scheme 1). The coupling was carried out in *N*-methyl-2-pyrrolidone (NMP) in the presence of 0.2 mol% of Pd/C (5 wt%) and K_2CO_3 at 120 °C. The reaction was stopped after 2 h resulting in 54% formation of *trans*-stilbene. In comparison, the reaction with only 0.4 mol% of 1,3-bis(2,6-diisopropylphenyl)-imidazolium chloride (IPr · HCl) additive yielded 73% of product under the same reaction conditions. The similar trend was observed when the reaction was carried out in DMF, although the process required a longer reaction time. The product yields were 30% without the use of additives and 70% with the addition of IPr · HCl salt, respectively.

There are two possible reasons underlying the effect of NPs modification. The first is associated with the positive influence of auxiliary ligands on stability of catalytically active species in the reaction mixture, *i.e.* NHC ligands on the NPs surface slow down the catalyst deactivation and prevent the precipitation of palladium black. The stabilizing role of NHC is not unknown.[16–20] The second reason concerns the fact that the presence of an auxiliary ligand changes the energy parameters of the catalytic cycle, facilitating the formation of the target product.[21–24] However, these assumptions require further research.

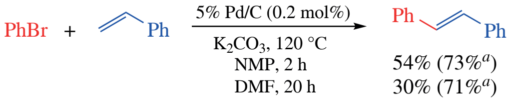

[a] IPr · HCl (0.4 mol%) was added

Scheme 1 Influence of IPr · HCl additive on Pd/C catalyzed Mizoroki–Heck coupling.

A leaching test was performed for the model reaction with IPr · HCl additive and without it. The reaction was carried out for 1 h, afterwards the solid and liquid phases were separated by centrifugation at 3500 rpm. The isolated sediments were washed and studied by TEM method (see Online Supplementary Materials, Figure S1). Analysis of the surface morphology changes for both catalytic systems revealed a significant decrease in the number of individual nanoparticles and the formation of 10–20 nm agglomerates in the post-reaction samples. The observed phenomenon can be attributed to palladium leaching and its subsequent redeposition onto the support surface.

The supernatant was additionally filtered through 0.45 μm syringe filter and transferred to a new reaction vessel containing the base since K_2CO_3 exhibits low solubility in NMP. Subsequent continuation of the reaction at 120 °C for 2 h led to a significant increase in the target product yield for the system containing the additive (from 50 to 81%). In contrast, the product yield in the additive-free system remained virtually unchanged (from 45 to 51%). The obtained results demonstrate that the presence of the NHC ligand in the system plays a stabilizing role for the catalytically active particles in solution.

To disclose the reasons underlying the catalyst modification effect, quantum chemical calculations were performed for the reaction between iodobenzene and methyl acrylate as model substrates (see Online Supplementary Materials for computational details). The Mizoroki–Heck reaction driven by ligand-free and NHC-modified Pd clusters was chosen as a model process. A dipalladium Pd_2 cluster with a fixed distance between metal atoms (2.74 Å) was taken as the model catalyst. The ligand-free cluster $Pd_2(THF)_4$ contains four solvate ligands which are necessary for saturation of the coordination sphere of Pd atoms, since the reaction occurs in the condensed phase. The model of the modified cluster $(IPr)Pd_2(THF)_2$ contained two solvate molecules, since bulky IPr ligand would displace two THF molecules.

The differences between the ligand-free and IPr-modified Pd_2 clusters become evident at the stage of iodobenzene coordination (Figure 1). In the ligand-free cluster **IIa**, the PhI molecule replaces one solvate molecule and coordinates *via* a double bond with one Pd atom. In contrast, in the IPr-modified cluster **IIb**, iodobenzene coordinates with two metal atoms. During the PhI coordination process (**Ib** → **IIb**), the IPr ligand shifts to a terminal position. An isomer with a bridged IPr and a terminal PhI also exists, but it is 4.3 kcal mol^{-1} less stable than **IIb**. The significant difference in the coordination energies of iodobenzene, amounting to 15.4 kcal mol^{-1}, is most likely due to the *trans* effect of the IPr ligand. The *trans*-positioned species NHC and PhI compete for the coordination sphere of the metal, leading to a destabilization of **IIb** compared to **IIa**.

At the next stage, methyl acrylate coordinates to the Pd^{II} atom of the dimer cluster (see Figure 1, **IV** → **V**). This process is energetically favorable for the ligand-free catalyst ($\Delta E = -4.6$ kcal mol^{-1}). The vacant coordination site of modified cluster **IVb** is shielded by the bulky IPr ligand. Displacing the IPr ligand to achieve the four-coordinated Pd^{II} atom structure **Vb** requires additional energy, making this stage energetically unfavorable ($\Delta E = 8.4$ kcal mol^{-1}). The destabilization of intermediate **Vb** facilitates the insertion of methyl acrylate into the Pd–Ph bond [$\Delta E^{\ddagger}$(**IVb** → **TS-VIb**) = 13.6 kcal mol^{-1}]. Conversely, the ligand-free dimer **Va** enters a shallow thermodynamic well, increasing the potential barrier for insertion step [$\Delta E^{\ddagger}$(**Va** → **TS-VIa**) = 17.7 kcal mol^{-1}].

The β-hydride elimination step (**VII** → **TS-VIII**) proceeds similarly for both catalytic systems and exhibits low activation energy (Figure 2). The resulting hydride products **IXa** and **IXb** are unstable and easily exchange the alkene ligand for the base molecule PhO^- (**IX** → **X**). As a result of the reductive elimination step, the coordination number of the Pd atom decreases. It can be hypothesized that the effect of the NHC ligand would be opposite to that observed during oxidative addition step. Indeed, this step

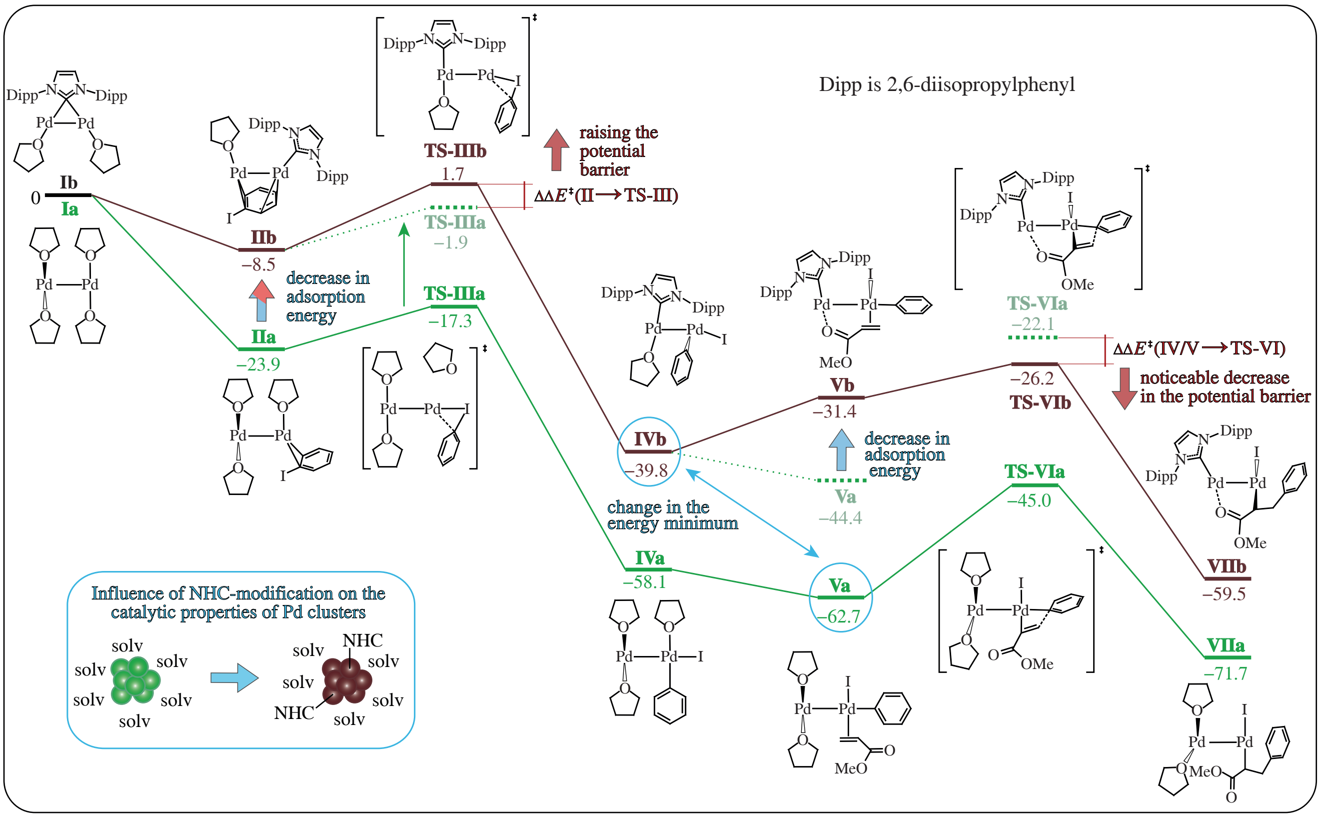

Figure 1 Reaction pathways of methyl acrylate phenylation on ligand-free (green PES) and IPr-modified (brown PES) Pd_2 clusters, free energies are given in kcal mol^{-1}. Part 1.

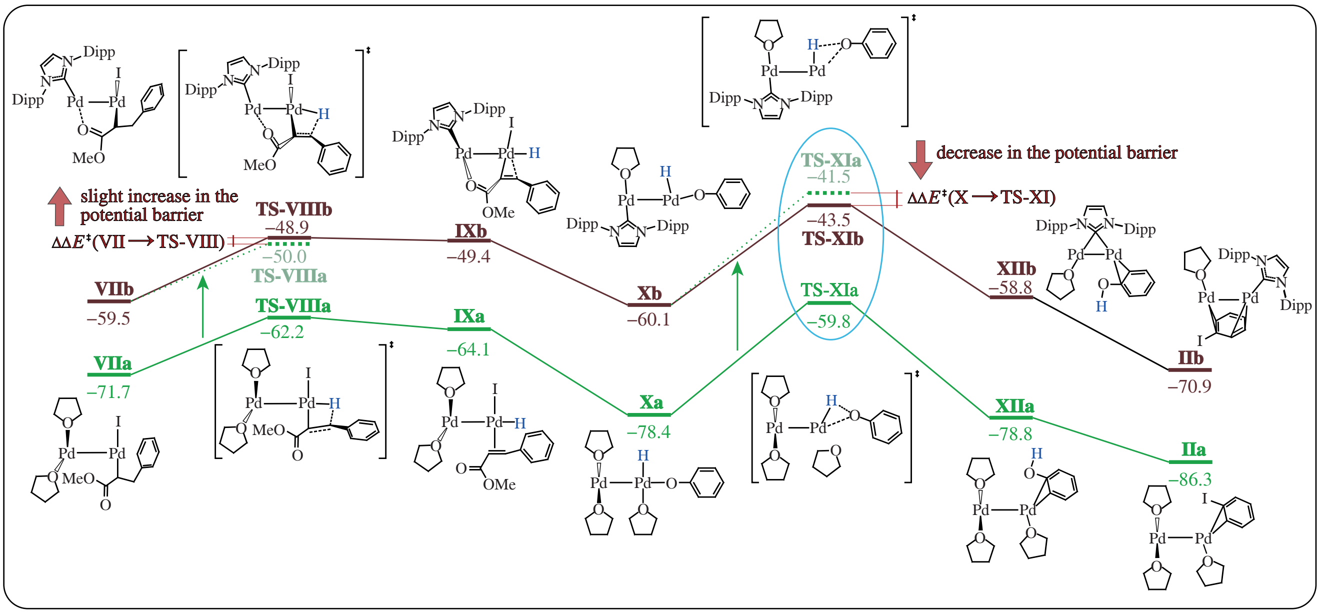

Figure 2 Reaction pathways of methyl acrylate phenylation on ligand-free (green PES) and IPr-modified (Dipp is 2,6-diisopropylphenyl, brown PES) Pd_2 clusters. Part 2.

proceeded more readily on the modified dimer [$\Delta E^{\ddagger}$(**Xb** → **TS-XIb**) = 16.6 kcal mol^{-1}] compared to the ligand-free catalyst [$\Delta E^{\ddagger}$(**Xa** → **TS-XIa**) = 18.6 kcal mol^{-1}]. Similar to the structure of **TS-IIIa**, the transition state **TS-XIa** lacks a Pd–THF bond. In structure **TS-XIb**, the corresponding coordination site remains vacant, shielded from the external environment by the bulky substituent of the IPr ligand. The effect of NHC modification was consistently observed in other model systems, including the Pd_1 metal complex and Pd_3–Pd_5 clusters (see Online Supplementary Materials, pages S4 and S5).

Catalytic performance of Pd-NHC/C catalytic system was evaluated in the Mizoroki–Heck reaction for various substrates (Scheme 2, Table 1). The syntheses were carried out for 4 h in NMP using K_2CO_3 as a base. Reaction of butyl acrylate with bromobenzene resulted in 90% yield of the $\beta(E)$ product (see Table 1, entry 1). Less reactive chlorobenzene does not react even during the prolonged reaction time at 140 °C (entry 2). In the case of utilization of 1-bromo-4-iodobenzene, the reaction selectively occurs at the iodine-substituted carbon atom (entry 3). Application of bulkier 1-bromonaphthalene had no negative influence on the reaction process and gives the similar yield of the target product (entry 4). Reactions with aryl bromides containing either electron withdrawing or electron donating substituents also proceed smoothly (entries 5–10). However, the presence of hydroxy substituent in *para*-position slows the reaction when only 33% of product was formed (entry 11). Moreover, introduction of methoxy or aldehyde groups in *para*- or *ortho*-positions in aryl bromide had crucial influence on the catalysis: no product was detected (entries 12–14), while full conversion into target products was observed in the reaction with the corresponding aryl iodides (entries 15–17). Surprisingly, utilization of *m*-bromoanisole gives 25% product yield (entry 18). The catalytic system was also tested on various alkenes (entries 19–23).

In summary, the addition of azolium salt to commercial Pd/C catalyst enhances its efficiency in the Mizoroki–Heck reaction. This additive acts as a NHC proligand thus modifying the metal surface. The Pd-NHC/C catalytic system was tested on a variety of aryl bromide and alkene substrates leading to the target products in moderate to quantitative yields. Split tests revealed the presence of leaching from the carbon support, which can result in the formation of low-nuclearity NHC-modified Pd species in solution. Quantum chemical calculations indicate that NHC-modification of the surface alters the energy profile of the reaction lowering the potential barriers for alkene insertion and reductive elimination stages. The approach to increasing the catalyst efficiency proposed in this work is not limited to Pd/C but can potentially be applied to more advanced catalytic systems.

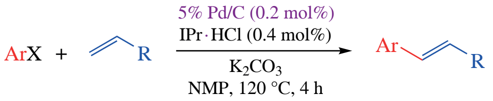

Scheme 2 The Mizoroki–Heck transformations catalyzed by NHC-modified palladium nanoparticles on carbon.

Table 1 Scope of the aryl halides and alkenes in the Mizoroki–Heck coupling.[a]

Entry	Ar	X	R	Product yield[b] (%)
1	Ph	Br	COOBu	90
2	Ph	Cl	COOBu	0
3	*p*-BrC_6H_4	I	COOBu	77
4	1-naphthyl	Br	COOBu	89
5	*p*-$Me_2NC_6H_4$	Br	COOBu	94
6	*p*-$H_2NC_6H_4$	Br	COOBu	77
7	*p*-MeC_6H_4	Br	COOBu	85
8	*p*-$MeC(O)C_6H_4$	Br	COOBu	79
9	*p*-$O_2NC_6H_4$	Br	COOBu	70
10	*m*-ClC_6H_4	Br	COOBu	99
11	*p*-HOC_6H_4	Br	COOBu	33
12	*p*-$MeOC_6H_4$	Br	COOBu	0
13	*o*-$MeOC_6H_4$	Br	COOBu	0
14	*o*-$HC(O)C_6H_4$	Br	COOBu	0
15	*p*-$MeOC_6H_4$	I	COOBu	99
16	*o*-$MeOC_6H_4$	I	COOBu	99
17	*o*-$HC(O)C_6H_4$	I	COOBu	99
18	*m*-$MeOC_6H_4$	Br	COOBu	25
19	Ph	Br	*p*-$MeOC_6H_4$	29
20	Ph	Br	Ph	97
21	Ph	Br	1-naphthyl	64
22	Ph	Br	*p*-ClC_6H_4	98
23	Ph	Br	Bn	33

[a] Conditions: ArX (1 equiv.), alkene (1.5 equiv.), 5% Pd/C (0.2 mol%), IPr · HCl (0.4 mol%), K_2CO_3 (1.6 equiv.), NMP, 120 °C, 4 h (see Scheme 2). [b] The yields were determined by ^{1}H NMR using *p*-dinitrobenzene as internal standard.

This study was financially supported by The Russian Science Foundation (grant no. 22-73-10109). This work was performed using the equipment in the Shared Research Center (Department of Structural Studies) of N. D. Zelinsky Institute of Organic Chemistry RAS, Moscow. The authors thank Dr. Alexey S. Galushko and Dr. Kirill S. Erokhin for the TEM measurements.

Online Supplementary Materials

Supplementary data associated with this article can be found in the online version at doi: 10.71267/mencom.7806.

References

1 C. Gao, F. Lyu and Y. Yin, *Chem Rev.*, 2020, **121**, 834; https://doi.org/10.1021/acs.chemrev.0c00237.

2 S. A. Kuznetsova, S. M. Yunusov, E. A. Khakina, A. V. Naumkin, D. A. Chusov, E. S. Kalyuzhnaya, M. M. Ilyin, Jr., V. V. Morozov, A. S. Kashin and Yu. N. Belokon, *Mendeleev Commun.*, 2024, **34**, 204; https://doi.org/10.1016/j.mencom.2024.02.014.

3 K. M. Appleby, E. Dzotsi, N. W. Scott, G. Dexin, N. Jeddi, A. C. Whitwood, N. E. Pridmore, S. Hart, S. B. Duckett and I. J. Fairlamb, *Organometallics*, 2021, **40**, 3560; https://doi.org/10.1021/acs.organomet.1c00452.

4 Y.-J. Fan, D. Wang, L. Wang and Y. Zhou, *Mendeleev Commun.*, 2023, **33**, 829; https://doi.org/10.1016/j.mencom.2023.10.030.

5 M. Koy, P. Bellotti, M. Das and F. Glorius, *Nat. Catal.*, 2021, **4**, 352; https://doi.org/10.1038/s41929-021-00607-z.

6 C. A. Smith, M. R. Narouz, P. A. Lummis, I. Singh, A. Nazemi, C.-H. Li and C. M. Crudden, *Chem. Rev.*, 2019, **119**, 4986; https://doi.org/10.1021/acs.chemrev.8b00514.

7 M. Ghosh and S. Khan, *ACS Catal.*, 2023, **13**, 9313; https://doi.org/10.1021/acscatal.3c01824.

8 D. J. Snelders, N. Yan, W. Gan, G. Laurenczy and P. J. Dyson, *ACS Catal.*, 2012, **2**, 201; https://doi.org/10.1021/cs200575r.

9 A. Yu. Kostyukovich, A. M. Tsedilin, E. D. Sushchenko, D. B. Eremin, A. S. Kashin, M. A. Topchiy, A. F. Asachenko, M. S. Nechaev and V. P. Ananikov, *Inorg. Chem. Front.*, 2019, **6**, 482; https://doi.org/10.1039/C8QI01095A.

10 V. M. Chernyshev, E. A. Denisova, D. B. Eremin and V. P. Ananikov, *Chem. Sci.*, 2020, **11**, 6957; https://doi.org/10.1039/D0SC02629H.

11 A. Yu. Kostyukovich, E. G. Gordeev and V. P. Ananikov, *Mendeleev Commun.*, 2022, **32**, 571; https://doi.org/10.1016/j.mencom.2022.09.001.

12 A. Yu. Kostyukovich, E. G. Gordeev and V. P. Ananikov, *Mendeleev Commun.*, 2023, **33**, 153; https://doi.org/10.1016/j.mencom.2023.02.002.

13 D. O. Prima, N. S. Kulikovskaya, R. A. Novikov, A. Yu. Kostyukovich, J. V. Burykina, V. M. Chernyshev and V. P. Ananikov, *Angew Chem., Int. Ed.*, 2024, **63**, e202317468; https://doi.org/10.1002/anie.202317468.

14 *The Mizoroki–Heck Reaction*, ed. M. Oestreich, Wiley, Chichester, 2009; https://content.e-bookshelf.de/media/reading/L-578263-0342690504.pdf.

15 M. Zhao, H. Liu, G. He, W. Zheng and J. Chen, *Mendeleev Commun.*, 2024, **34**, 212; https://doi.org/10.1016/j.mencom.2024.02.017.

16 A. Rühling, K. Schaepe, L. Rakers, B. Vonhören, P. Tegeder, B. J. Ravoo and F. Glorius, *Angew Chem., Int. Ed.*, 2016, **55**, 5856; https://doi.org/10.1002/anie.201508933.

17 F. P. Da Silva, J. L. Fiorio and L. M. Rossi, *ACS Omega*, 2017, **2**, 6014; https://pubs.acs.org/doi/10.1021/acsomega.7b00836.

18 L. S. Ott, M. L. Cline, M. Deetlefs, K. R. Seddon and R. G. Finke, *J. Am. Chem. Soc.*, 2005, **127**, 5758; https://doi.org/10.1021/ja0423320.

19 M. Planellas, R. Pleixats and A. Shafir, *Adv. Synth.*, 2012, **354**, 651; https://doi.org/10.1002/adsc.201100574.

20 M. Planellas, Y. Moglie, F. Alonso, M. Yus, R. Pleixats and A. Shafir, *Eur. J. Org. Chem.*, 2014, **2014**, 3001; https://doi.org/10.1002/ejoc.201400162.

21 J. B. Ernst, C. Schwermann, G. I. Yokota, M. Tada, S. Muratsugu, N. L. Doltsinis and F. Glorius, *J. Am. Chem. Soc.*, 2017, **139**, 9144; https://doi.org/10.1021/jacs.7b05112.

22 P. Tegeder, M. Marelli, M. Freitag, L. Polito, S. Lamping, R. Psaro, F. Glorius, B. J. Ravoo and C. Evangelisti, *Dalton Trans.*, 2018, **47**, 12647; https://doi.org/10.1039/C8DT02535E.

23 C. Yue, Q. Xing, P. Sun, Z. Zhao, H. Lv and F. Li, *Nature Commun.*, 2021, **12**, 1875; https://doi.org/10.1038/s41467-021-22084-5.

24 H. Min, H. Miyamura and S. Kobayashi, *Chem. Lett.*, 2016, **45**, 837; https://doi.org/10.1246/cl.160369.

Received: 22nd April 2025; Com. 25/7806